Tuberculosis 118 (2019) 101853

Contents lists available at ScienceDirect

Tuberculosis

journal homepage: www.elsevier.com/locate/tube

Non-Tuberculous Mycobacteria: General

In silico and *in vitro* evaluation of tetrahydropyridine compounds as efflux inhibitors in *Mycobacterium abscessus*

Ivy B. Ramis[a], Júlia S. Vianna[a,*], Lande Silva Junior[a,d], Andrea von Groll[a], Daniela F. Ramos[a], Marcio Marçal Lobo[b], Nilo Zanatta[b], Miguel Viveiros[c], Pedro E. Almeida da Silva[a]

[a] *Núcleo de Pesquisa Em Microbiologia Médica, Universidade Federal de Rio Grande, Rua General Osório s/n, Rio Grande, RS, Brazil*
[b] *Núcleo de Química de Heterociclos, Departamento de Química, Universidade Federal de Santa Maria, Santa Maria, Brazil*
[c] *Unidade de Microbiologia Médica, Global Health and Tropical Medicine, GHTM, Instituto de Higiene e Medicina Tropical, IHMT, Universidade NOVA de Lisboa, UNL, Lisboa, Portugal*
[d] *Instituto Federal Sul-rio-grandense, Pelotas, RS, Brazil*

ARTICLE INFO

Keywords:
Mycobacteria
efflux
Drug resistance
Tetrahydropyridine
Molecular modeling

ABSTRACT

Herein, we evaluated tetrahydropyridine (THP) compounds (NUNM) as antimicrobials and inhibitors of the efflux mechanism in *M. abscessus*. subsp. *abscessus*. The modulation factor (MF) of efflux inhibitors was calculated from the minimum inhibitory concentrations (MICs) of amikacin (AMI), ciprofloxacin (CIP) and clarithromycin (CLA) in the absence and presence of subinhibitory concentrations of the NUNM compounds and canonical inhibitors carbonyl cyanide *m*-chlorophenyl hydrazone (CCCP) and verapamil (VP). The kinetics of the intracellular accumulation of the fluorimetric substrate ethidium bromide (EtBr) was evaluated and calculated by the relative final fluorescence (RFF). In addition, molecular modeling simulations for the MmpL5 and Tap efflux transporters with ligands (CLA, NUNM, CCCP, VP and EtBr) were performed to better understand the efflux mechanism. We highlight the NUNM01 compound because it reduced the MICs of AMI, CIP and CLA by 4-, 4- and 16-fold, respectively, had the highest effect on EtBr accumulation (RFF = 3.1) and showed a significant *in silico* affinity for the evaluated proteins in docking simulations. Based on the analyses performed *in vitro* and *in silico*, we propose that NUNM01 is a potential pharmacophore candidate for the development of a therapeutic adjuvant for *M. abscessus* infections.

1. Introduction

Pulmonary and extrapulmonary infections caused by *Mycobacterium abscessus* are difficult to treat, especially because of its high level of acquired and intrinsic antimicrobial resistance, which results in limited therapeutic options and multiple treatment failures [1,2].

Clarithromycin (CLA) is the main antimicrobial of the therapeutic regimen for *M. abscessus* infections; however, acquired resistance, mainly related to mutations in the *rrl* gene, may occur. Another resistance mechanism developed by *M. abscessus* to CLA is an inducible resistance conferred by the *erm* (41) gene that codes a methyltransferase [3,4]. In addition to *erm* (41), CLA can also induce several genes that code for efflux pumps. Therefore, it is possible that the overexpression of *erm* (41) and the overexpression of efflux genes work synergically to determine resistant phenotypes of *M. abscessus* [5,6].

Despite the scarce knowledge of which pumps are involved in drug efflux in *M. abscessus*, a recent study demonstrated that high levels of drug resistance in *M. abscessus* can be achieved through mechanisms of efflux involving the transporter MmpL5, belonging to family RND (resistance nodulation division) [7]. Also, it was detected in clinical samples of *M. abscessus* the overexpression of *tap* efflux pump genes that belong to MFS (major facilitator superfamily) [8].

The induction of efflux pumps has been recognized as the first step in a general pathway to drug resistance in microorganisms in general [9]. Hence, inhibition of efflux by compounds that act as efflux inhibitors (EI) is a promising alternative to increase the activity of antimicrobials [10,11].

Tetrahydropyridines (THP) have shown therapeutic and pharmacological properties as flow regulators of calcium ions and can be candidates for EI in bacteria [12]. Recently, we showed that a THP compound exhibits potent efflux inhibitory activity in *Escherichia coli*. Docking studies showed that the mechanism of action of this inhibition could entail competition with substrate for binding sites [13].

Molecular docking studies help to elucidate the interaction between

* Corresponding author.
E-mail address: jusvianna@hotmail.com (J.S. Vianna).

https://doi.org/10.1016/j.tube.2019.07.004
Received 19 February 2019; Received in revised form 18 July 2019; Accepted 22 July 2019
Available online 23 July 2019

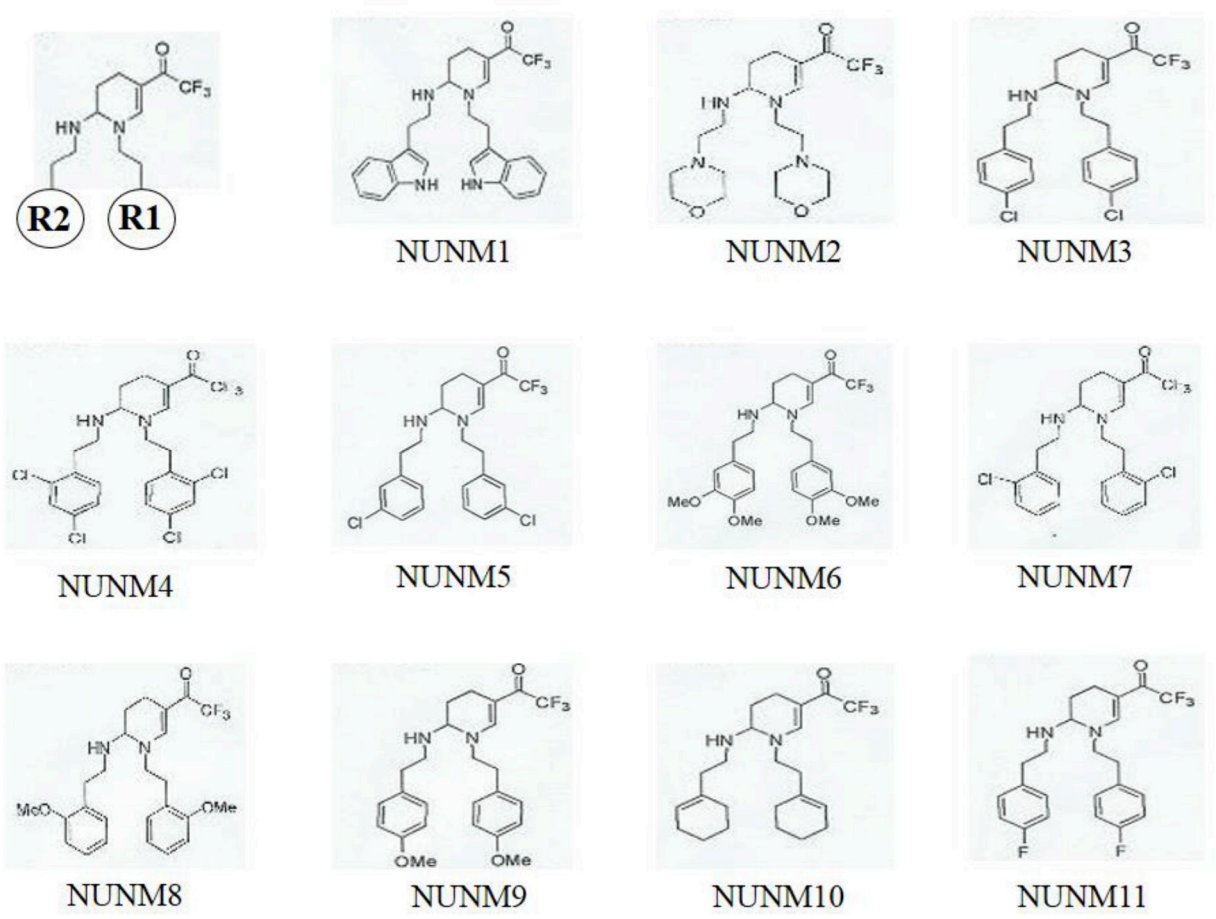

Fig. 1. Structure of 11 tetrahydropirydines compounds.

Table 1
Minimum inhibitory concentrations of the antimicrobials, efflux inhibitors, and ethidium bromide against *M. abscessus* subsp. *abscessus* (ATCC 19977).

	M. abscessus ATCC 19977 MIC (μg/mL)
AMI	1.0
CIP	1.0
CLA[a]	0.5
CLA[b]	2.0
CLA[c]	4.0
CCCP	0.4
VP	312.5
NUNM 01	100
NUNM 02	> 200
NUNM 03	25
NUNM 04	25
NUNM 05	50
NUNM 06	> 200
NUNM 07	50
NUNM 08	100
NUNM 09	100
NUNM 10	25
NUNM 11	100
EtBr	8.0

MIC Minimum inhibitory concentration, AMI amikacin, CIP ciprofloxacin, CLA clarithromycin, CCCP Carbonyl cyanide *m*-chlorophenyl hydrazone, VP verapamil, EtBr ethidium bromide. a value by visual reading in day 3, b value by visual reading in day 5, c value by visual reading in day 7.

compounds and a target receptor, through many orientations and conformations. The best position and conformation of the drug candidate is estimated by the free energy of binding (FEB) scores - the more negative the FEB, the stronger the binding [14].

Table 2
Interaction between the efflux inhibitors in combination with antimycobacterial drugs against *M. abscessus* subsp. *abscessus* (ATCC 19977).

	MIC (μg/mL)	MF		MIC (μg/mL)	MF		MIC (μg/mL)	MF
AMI	1.0	–	CIP	1.0	-	CLA	4.0[c]	-
CCCP	0.5	2	CCCP	0.5	2	CCCP	1.0	4
VP	0.25	4	VP	0.5	2	VP	4.0	1
NUNM01	0.25	4	NUNM01	0.25	4	NUNM01	0.25	16
NUNM03	0.5	2	NUNM03	0.5	2	NUNM03	4.0	1
NUNM04	1.0	1	NUNM04	1.0	1	NUNM04	4.0	1
NUNM05	0.5	2	NUNM05	0.5	2	NUNM05	2.0	2
NUNM07	1.0	1	NUNM07	1.0	1	NUNM07	4.0	1
NUNM08	0.5	2	NUNM08	1.0	1	NUNM08	0.5	8
NUNM09	0.5	2	NUNM09	0.5	2	NUNM09	0.25	16
NUNM10	0.5	2	NUNM10	1.0	1	NUNM10	4.0	1
NUNM11	0.5	2	NUNM11	0.5	2	NUNM11	0.5	8

MIC Minimum inhibitory concentration, MF modulation factor, AMI amikacin, CIP ciprofloxacin, CLA clarithromycin, CCCP Carbonyl cyanide *m*-chlorophenyl hydrazone, VP verapamil. c MIC value by visual reading in day 7.

Herein, we evaluated 11 THP compounds as antimicrobials and inhibitors of efflux in *M. abscessus* and compared the performance of the THP compounds versus the canonical EI, carbonyl cyanide *m*-chlorophenyl hydrazone (CCCP) and verapamil (VP). Additionally, molecular modeling simulations for the *M. abscessus* protein transporters MmpL5 and Tap were performed to provide a better comprehension of the efflux mechanism.

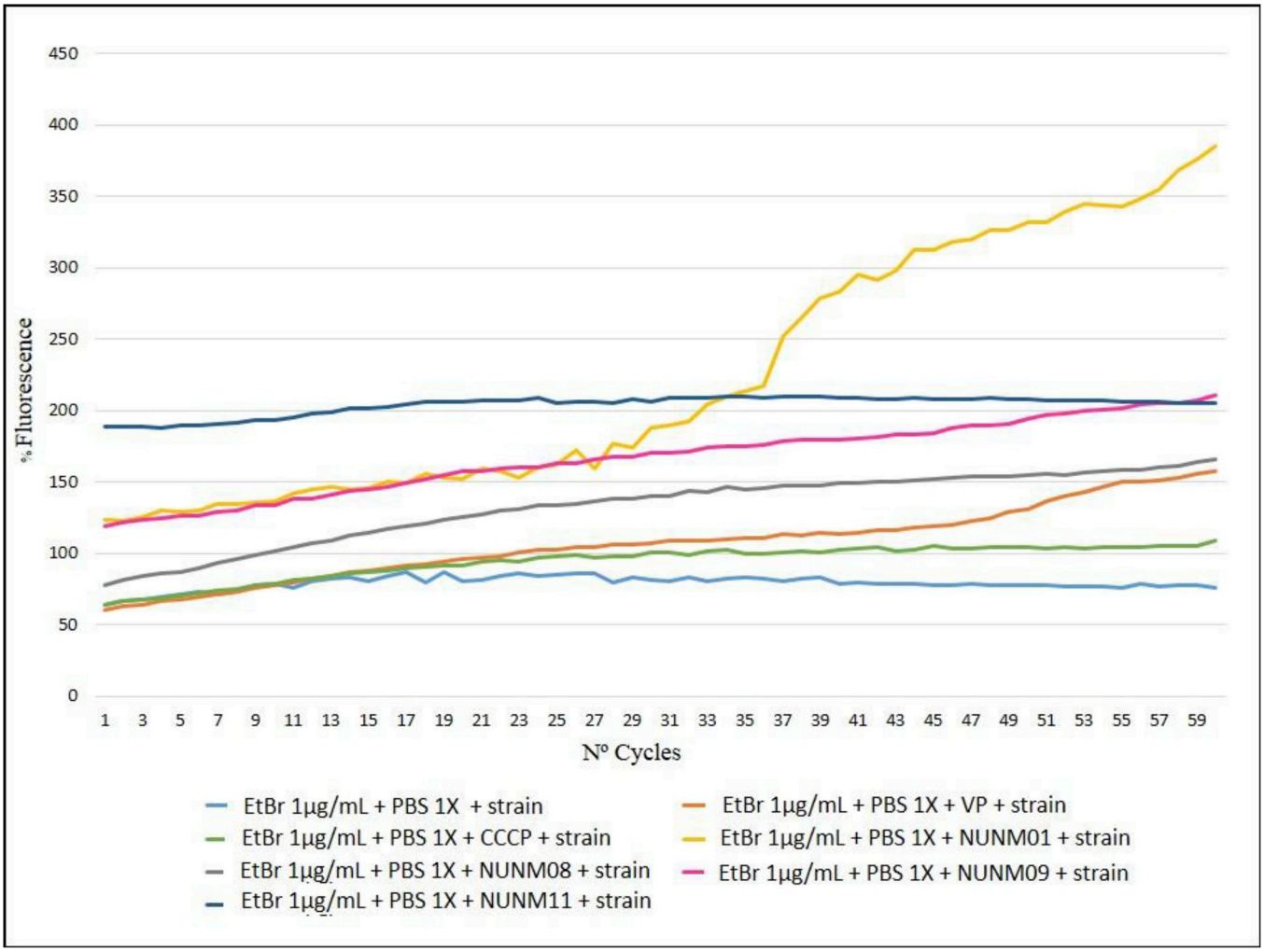

Fig. 2. Effect of the efflux inhibitors (Carbonyl cyanide *m*-chlorophenyl hydrazine – CCCP, Verapamil - VP) and tetrahydropyridine compounds (NUNM01, NUNM08, NUNM09 and NUNM11) on the accumulation of ethidium bromide (EtBr) in *M. abscessus* subsp. *abscessus* (ATCC 19977). The graphic shows the accumulation of EtBr in the presence of efflux inhibitors.

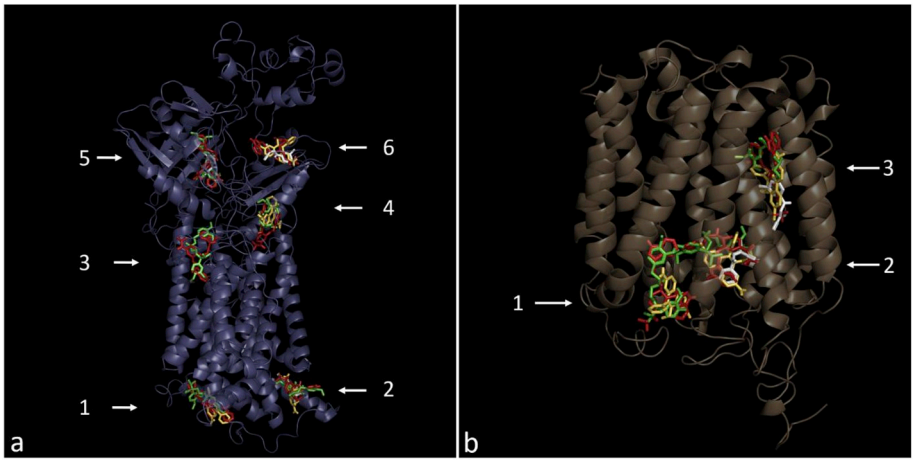

Fig. 3. Blind docking. Six sites of high free energy of binding for the ligands at MmpL5 (a) (blue cartoon) and three for Tap (b) (light brown cartoon). The ligands are represented as colored sticks: NUNM01 (red), carbonyl cyanide *m*-chlorophenyl hydrazine (white), verapamil (green), ethidium bromide (yellow). (For interpretation of the references to color in this figure legend, the reader is referred to the Web version of this article.)

2. Methodology

2.1. Strain and bacterial suspension

We used the reference strain *M. abscessus* subsp. *abscessus* (ATCC 19977). The strain was cultured on Ogawa-Kudoh medium and incubated at 37 °C for 2–15 days. The inoculum was prepared according to the CLSI guidelines in distilled water, adjusted to a McFarland tube no. 0.5, and diluted 1:10 in the medium used to perform the broth microdilution method (Mueller-Hinton) [15].

Table 3
Free Energy of Binding (FEB) for the ligands at the respective binding sites found by blind docking assays at MmpL5 and Tap models.

Binding Site	Ligands and Free Energy of Binding (FEB) (kcal/mol)						
	MmpL5						
	NUNM01	NUNM11	NUNM08	NUNM09	VP	CCCP	EtBr
1	−9.1	−7.2	−6.5	−6.4	−6.5	NC	−6.8
2	−9.9	−9.1	−8.3	−8.7	−6.2	−6.2	−7.9
3	−9.6	−8.6	−8.6	−7.4	−6.6	NC	NC
4	−10.6	−8.5	−8.5	−8.0	−6.8	−6.3	−7.8
5	−9.7	−8.9	−9.0	−8.4	−8.5	−6.7	NC
6	−9.4	−8.4	−8.3	−7.9	NC	−6.4	−7.7
Tap							
1	−10.3	−9.6	−8.8	−8.4	−7.6	NC	−8.6
2	−10.2	−9.7	−9.2	−8.3	−7.2	−6.9	−8.6
3	−11.4	−10.1	−9.4	−8.4	−8.0	−6.7	−8.7

NC No-correspondence.

2.2. Antimicrobials and efflux inhibitors

Amikacin (AMI), ciprofloxacin (CIP), CLA, carbonyl cyanide *m*-chlorophenyl hydrazone (CCCP) and verapamil (VP) were purchased from Sigma-Aldrich (St. Louis, MO, USA) and were solubilized according to the manufacturer's recommendations. AMI and VP were prepared in distilled water. CIP was prepared in 0.05 N HCl (dilute aqueous acid). CLA and CCCP were prepared in dimethyl sulfoxide (DMSO). Stock solutions were stored at −20 °C. Working solutions were prepared in Mueller-Hinton (MH) broth on the day of each experiment.

2.3. Tetrahydropyridine compounds

Eleven synthetic tetrahydropyridine compounds were obtained according to a method described previously [16] (Fig. 1). All were solubilized in 99.5% DMSO at a concentration of 10 mg/mL and stored at 4 °C.

2.4. Determination of minimum inhibitory concentration (MIC)

The MICs of antimicrobials and EI were determined using the broth 96-well microtiter plate microdilution method according to CLSI (2011), with some modifications. Briefly, serial two-fold dilutions of each antimicrobial were prepared directly in the plate containing 100 µl of MH broth and, later, 100 µl of inoculum diluted 1:10, was added to each well. The inoculated plates were incubated at 37 °C in a normal atmosphere, under aerobiose conditions, for 48 h. Subsequently, 30 µl of 0.02% resazurin was added to each well, and the plate was incubated under aerobiose conditions overnight at 37 °C for color development. Resazurin was used as a cell viability indicator and bacterial growth was evidenced when the color changed from blue (oxidized state) to pink (reduced state) [17]. The MIC was defined as the lowest drug concentration that inhibited bacterial growth at day 3 [18]. In each plate tested, a growth control (inoculum without antimicrobial) and a sterile control (only medium) were included. In addition, to detect CLA induced resistance, the plates were incubated for 14 days. The strain was considered susceptible when the MIC was less than or equal to 2 µg/mL and resistant when above that on day 3. However, when the strain was susceptible on day 3 and resistant after day 5, they was considered induced resistant [6]. All assays were carried out in triplicate.

2.5. Cytotoxicity assay

NUNM compound toxicity was assessed in metabolically active cells compared to untreated cells using the cell line J774A.1 (ATCC TIB-67). The macrophages were maintained in DMEM (Vitrocell Embriolife) supplemented with 10% FBS and 1% antibiotic and antimycotic and incubated at 37 °C in a moist atmosphere (5% CO_2) until reaching 80% confluence. The cytotoxicity assay was performed in a 96-well microplate at a density of 1×10^5 cells/mL. After incubating for 24 h, cells were treated with compounds ranging from 200 to 0.8 µg/mL and again incubated for 24 h. Next, 30 µL of resazurin (0.01%) were added to each well, the plate was incubated overnight, and the IC_{50} (concentration that inhibited 50% of cell growth) was determined via fluorescence measurement using a spectrophotometer at 620 nm [19,20]. The inhibition (%) of cell proliferation, at each concentration was determined as follows: inhibitory growth = (1-Abs600 treated cells/Abs600 control cells) × 100).

2.6. Modulatory effect of efflux inhibitors on antimicrobial activity

The MICs of AMI, CIP and CLA were determined in the absence and presence of a subinhibitory concentration (½ MIC) of the canonical inhibitors (CCCP and VP) and the THP compounds. Modulation factor (MF) was used to quantify the effects of EI on the MICs of AMI, CIP and CLA using the formula: MF = MIC antimicrobial/MIC antimicrobial + EI [21]. The MF reflects the reduction in MIC values of a given antimicrobial in the presence of the EI, which is considered significant when MF ≥ 4 (four-fold reduction) [22]. These assays were performed in triplicate.

2.7. Semi-automated fluorometric method

The method was performed using an Infinite F200 fluorometer (Tecan) to monitor ethidium bromide (EtBr) accumulation. Fluorescence was acquired in 60 cycles of 90 s at 37 °C. The excitation and emission wavelengths were 530 and 580 nm, respectively. Accumulation assays were conducted in triplicate as described by Ramis et al. (2018) [23]. Briefly, the strains were grown in 10 mL of MH with 5% OADC supplement (oleic acid/albumin/dextrose/catalase) (Becton and Dickinson, Diagnostic Systems) and 0.05% Tween 80 at 37 °C until they reached a 600-nm optical density ($O.D._{600}$) of 0.8. Cells were washed by centrifugation at 2300 g for 3 min, then the supernatant was discarded and the pellet was washed in phosphate-buffered solution (PBS) 1x. To determine the EtBr concentration that established equilibrium between efflux and influx, we added 50 µL of bacterial suspension and 50 µL of EtBr to a 96-well black plate in different concentrations ranging from 0.63 to 3,17 µM. The selected EtBr concentration was used to evaluate the EI's capacity to retain ethidium bromide inside the cells. The EIs were tested at sub-inhibitory concentrations (½ MIC) to assess their inhibitory ability against efflux systems in *M. abscessus*. We also added control wells containing only

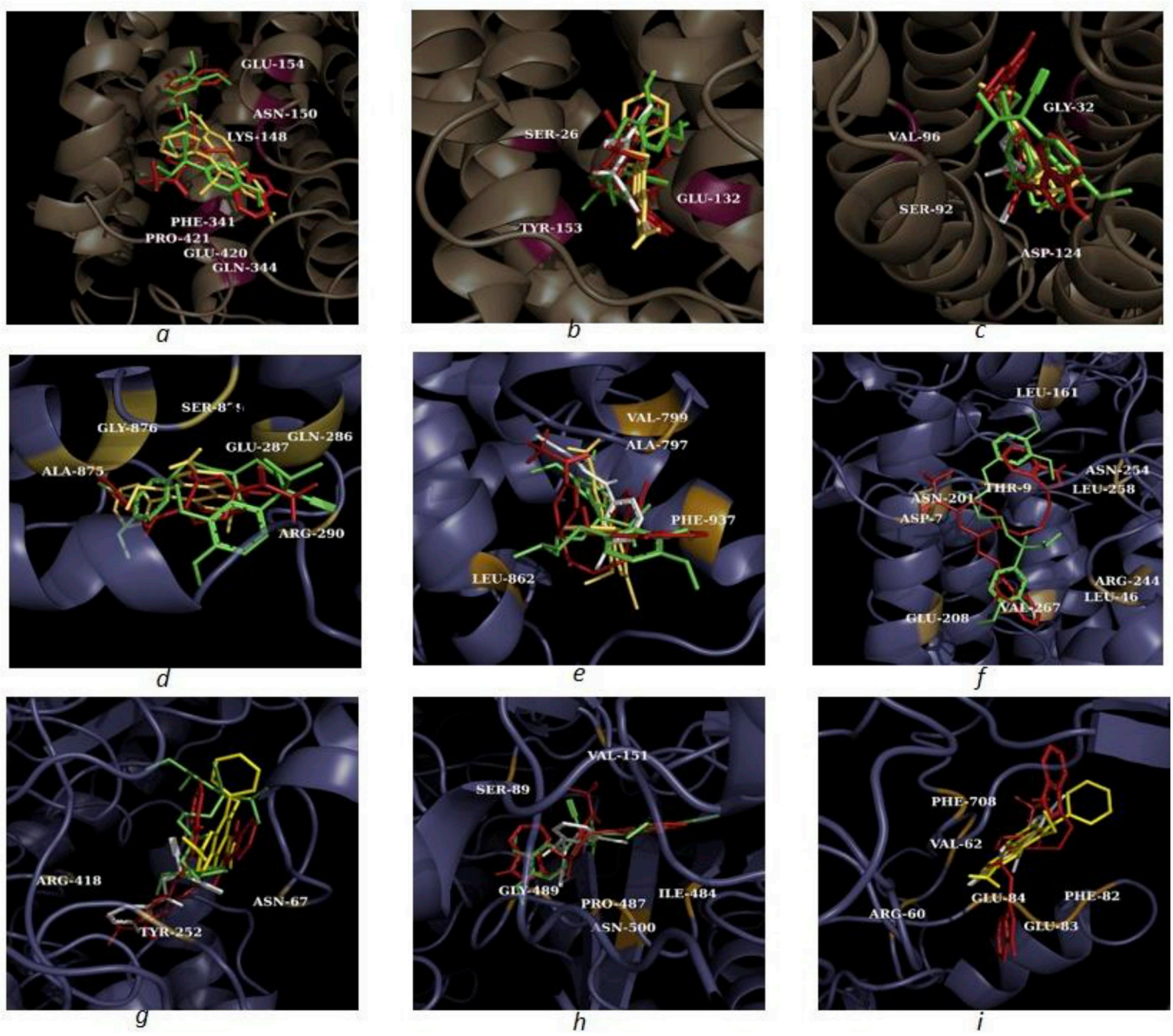

Fig. 4. Blind docking. Binding sites at Tap (*a* site 1, *b* site 2 and *c* site 3) (light brown cartoon), and MmpL5 (*d* site 1, *e* site 2, *f* site 3, *g* site 4, *h* site 5 and *I* site 6) (blue cartoon) for NUNM01 (red), carbonyl cyanide *m*-chlorophenyl hydrazine (white), verapamil (green), ethidium bromide (yellow). Some of the protein residues contacted by the ligands depicted in orange (Tap) and pink (MmpL5) are listed for the respective panels (refer to Tables 5 and 6 for a complete list): a) LYS lysine 148, ASN aspargine 150, GLU glutamic acid 154, PHE phenylalanine 341, GLN glutamine 344, GLU glutamic acid 420, PRO proline 421; b) SER serine 26, GLU glutamic acid 132, TYR tyrosine 153; c) GLY glycine 32, SER serine 92, VAL valine 96, ASP aspartic acid 124; d) GLN glutamine 286, GLU glutamic acid 287, ARG arginine 290, ALA alanine 875, GLY glycine 876, SER serine 879; e) ALA alanine 797, VAL valine 799, LEU leucine 862, PHE phenylalanine 937; f) ASP aspartic acid 7, THR threonine 9, LEU leucine 46, LEU leucine 161, ASN aspargine 201, GLU glutamic acid 208, ARG arginine 244, ASN aspargine 254, LEU leucine 258, VAL valine 267. (For interpretation of the references to color in this figure legend, the reader is referred to the Web version of this article.)

EtBr and bacterial suspension [24,25]. The EI inhibitory activity was determined by calculating the RFF value using the formula: RFF = $RF_{treated} - RF_{untreated}/RF_{untreated}$, where.

$RF_{treated}$ corresponds to the relative fluorescence at the last time point of the EtBr retention curve in the presence of EI and $RF_{untreated}$ corresponds to the relative fluorescence at the last time point of the EtBr accumulation curve of the untreated control well. The major difference between $RF_{treated}$ and $RF_{untreated}$ the greater the degree of EtBr accumulation is [24,25]. An RFF above zero indicates that the cells accumulate more EtBr under the condition used than the control (untreated) cells do. Negative RFF values indicate that the treated cells accumulated less EtBr than the controls do [26].

2.8. Computer simulations

The FASTA sequences for the efflux proteins MmpL5 and Tap (966 and 423 amino acids, respectively), from *M. abscessus* subsp. *abscessus*, were accessed at GenBank [27] (locus identifiers SLK97379.1 and SIJ44512.1, respectively) [28,29]. The three dimensional protein models were obtained through homology modeling with Phyre2 [30], a web based tool for protein structure prediction. The modeling mode was set to "intense". The 3D model for MmpL5 had 91% of residues modeled with a confidence level higher than 90%, while Tap had 100% of residues modeled with more than 90% confidence. Afterwards, both biomolecular structures were electrically neutralized and then solvated in a truncated octahedron water box, using xLeap from AmberTools14 [31].

Table 4
Free Energy of Binding (FEB) for the ligands at the respective binding sites found by slice docking assays at MmpL5 and Tap models.

Binding Site	Ligands and Free Energy of Binding (FEB) (kcal/mol)							
	MmpL5							
	NUNM01	NUNM11	NUNM08	NUNM09	CLA	VP	CCCP	EtBr
1	−8.1	−6.4	−7.0	−7.1	−7.9	−6.7	NC	−6.8
2	−8.4	NC	−6.7	NC	−6.7	−6.4	NC	−6.4
3	−9.7	−9.0	−8.0	−7.6	−7.7	−6.6	−5.6	−6.4
4	NC	NC	NC	NC	−7.3	NC	NC	NC
5	−9.3	−8.2	−8.1	−7.6	−6.8	−6.9	−5.6	−6.2
6	NC	NC	−8.1	−7.6	−7.0	−5.9	NC	−7.1
7	−9.3	−7.9	−7.3	−7.6	−7.1	−5.7	NC	−6.7
8	−9.3	−8.0	−7.7	−7.6	−8.0	−6.6	−5.1	−6.9
Tap								
1	−6.8	−6.0	−6.5	−6.0	−6.4	−6.3	−4.6	−6.1
2	−7.2	−6.3	−6.6	−6.0	−6.9	−6.5	−5.2	NC
3	−10.3	−8.6	−9.0	−8.5	−8.8	−7.8	−6.9	−7.6
4	NC	NC	NC	NC	−5.9	NC	NC	−7.2
5	−9.9	−8.6	−8.4	−8.1	−6.8	−6.6	−5.8	−7.2

NC No-correspondence.

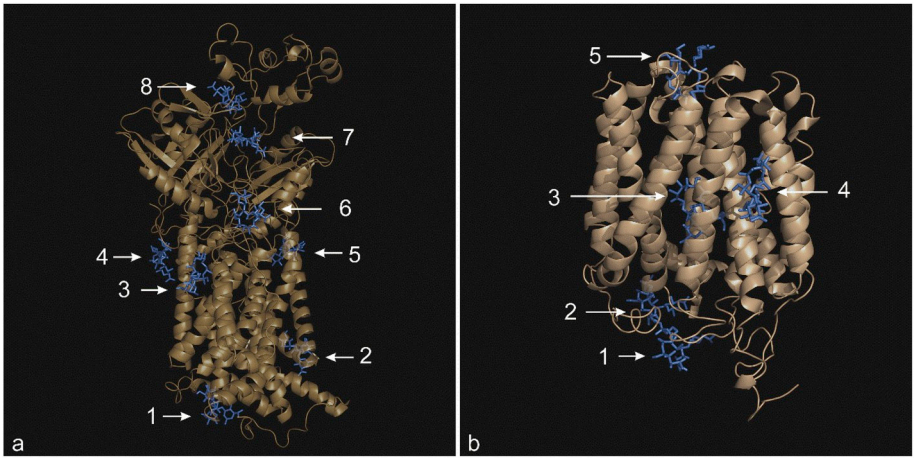

Fig. 5. Slice docking: Eight sites of high free energy of binding for CLA at MmpL5 (a) and five at Tap (b), both models are in the cartoon representation. Clarithromycin is depicted as blue sticks. (For interpretation of the references to color in this figure legend, the reader is referred to the Web version of this article.)

Table 5
Blind docking. Protein residues contacted by the ligands NUNM01, verapamil, ethidium bromide and carbonyl cyanide *m*-chlorophenyl hydrazone at the binding sites on MmpL5.

Blind Docking – MmpL5											
	Site 1				Site 4				Site 6		
NUNM01	VP	EtBr	CCCP	NUNM01	VP	EtBr	CCCP	NUNM01	VP	EtBr	CCCP
GLY 372	X	–	–	GLN 52	X	X	–	ARG 60	–	X	X
GLN 286	X	X	X	MET 59	X	–	–	VAL 62	–	X	X
GLU287	X	X	–	MET 64	X	X	–	PHE 82	–	X	X
ARG 290	X	X	–	PRO 66	X	X	–	GLU 83	–	X	X
ARG 380	X	–	–	SER 65	–	X	–	GLU 84	–	X	X
ARG 872	X	–	–	ALA 69	X	X	–	ILE 492	–	X	–
ALA 875	X	X	–	ASN 67	X	X	X	ILE 705	–	X	–
GLY 876	X	X	–	ALA 71	X	X	–	LYS 706	–	X	X
SER 879	X	X	X	TYR 252	X	X	X	PHE 708	–	X	X

(*continued on next page*)

Table 5 (*continued*)

Blind Docking – MmpL5											
	Site 1				Site 4				Site 6		
NUNM01	VP	EtBr	CCCP	NUNM01	VP	EtBr	CCCP	NUNM01	VP	EtBr	CCCP
ALA 963	–	X	–	HIE 253	X	–	X				
ALA964	–	X	–	GLY 257	–	–	X				
ALA 966	–	X	–	PRO 330	–	–	X				
	Site 2			TYR 331	–	–	X				
NUNM01	VP	EtBr	CCCP	PHE 332	–	–	X				
ARG 796	X	–	–	LYS 333	–	–	X				
ALA 797	X	X	X	THR 334	–	–	X				
VAL 799	X	X	X	ARG 418	X	X	X				
ALA 800	–	X	X		Site 5						
VAL 855	X	–	X	NUNM01	VP	EtBr	CCCP				
LYS 859	X	X	–	VAL 56	–	–	X				
LEU 862	X	X	X	SER 88	X	–	–				
LEU 933	X	–	X	SER 89	X	–	X				
GLY 934	X	X	–	VAL 91	X	–	–				
PHE 937	X	X	X	ILE 93	X	–	–				
ARG 948	X	X	–	GLN 127	X	–	–				
	Site 3			ASP 128	X	–	–				
NUNM01	VP	EtBr	CCCP	ALA 138	X	–	–				
ASP 7	X	–	–	GLN140	X	–	–				
THR 9	X	–	–	VAL 151	X	–	X				
LEU 46	X	–	–	LEU 447	X	–	–				
LEU 161	X	–	–	ILE 484	X	–	X				
ASN 201	X	–	–	PRO 487	X	–	X				
GLU 208	X	–	–	GLY 489	X	–	X				
ARG 244	X	–	–	ASN 500	X	–	X				
ASN 254	X	–	–	SER 502	X	–	–				
LEU 258	X	–	–	GLN 540	X	–	–				
VAL 267	X	–	–	GLU 548	X		–				

The residues contacted by NUNM01 are listed at the first column, the "X", if present, indicates that the other compounds also contact these residues. CCCP Carbonyl cyanide *m*-chlorophenyl hydrazone, VP verapamil, EtBr ethidium bromide, ALA alanine, ARG arginine, ASN aspargine, ASP aspartic acid, GLY glycine, GLN glutamine, GLU glutamic acid, HIE histidine, ILE isoleucine, LEU leucine, LYS lysine, ET methionine, PHE phenylalanine, PRO proline, SER serine, THR threonine, TYR tyrosine, VAL valine.

Table 6
Blind Docking. Protein residues contacted by the ligands NUNM01, verapamil, ethidium bromide and carbonyl cyanide *m*-chlorophenyl hydrazone at the binding sites on Tap.

Blind Docking – Tap											
	Site 1				Site 2				Site 3		
NUNM01	VP	EtBr	CCCP	NUNM01	VP	EtBr	CCCP	NUNM01	VP	EtBr	CCCP
ASP 147	X	–	–	LEU 22	–	X	X	GLY 32	X	X	X
LYS 148	X	X	–	ALA25	–	–	X	SER 36	X	X	–
ASN 150	X	X	–	SER 26	X	X	X	ALA 39	X	–	–
GLU 154	X	X	–	ALA29	X	X	–	LEU 40	X	–	–
ALA 282	X	–	X	ARG 131	X	–	X	GLY 61	X	–	–
TYR 285	X	–	X	GLU 132	X	X	X	SER 92	X	–	X
GLY 333	X	–	X	LEU 135	–	X	X	VAL 96	X	X	X
PRO 337	–	X	X	ASN 150	–	X	X	ILE 99	X	–	–
PHE 341	X	X	–	TYR 153	X	X	X	ALA 117	X	X	–
GLN 344	X	X	–	GLU 154	X	–	–	ALA 121	X	X	–
GLU 420	X	X	–	PHE 157	X	X	–	ASP124	X	X	X
PRO 421	X	X	–	ASN 158	X	–	–	THR 180	X	X	–
ARG 423	X	–	–	TYR 332	X	–	–	VAL 183	X	X	–
				ASN 340	X	–	–				

The residues contacted by NUNM01 are listed at the first column, the "X", if present, indicates that the other compounds also contact these residues. CCCP Carbonyl cyanide *m*-chlorophenyl hydrazone, VP verapamil, EtBr ethidium bromide, ALA alanine, ARG arginine, ASN aspargine, ASP aspartic acid, GLY glycine, GLN glutamine, GLU glutamic acid, ILE isoleucine, LEU leucine, LYS lysine, PHE phenylalanine, PRO proline, SER serine, THR threonine, TYR tyrosine, VAL valine.

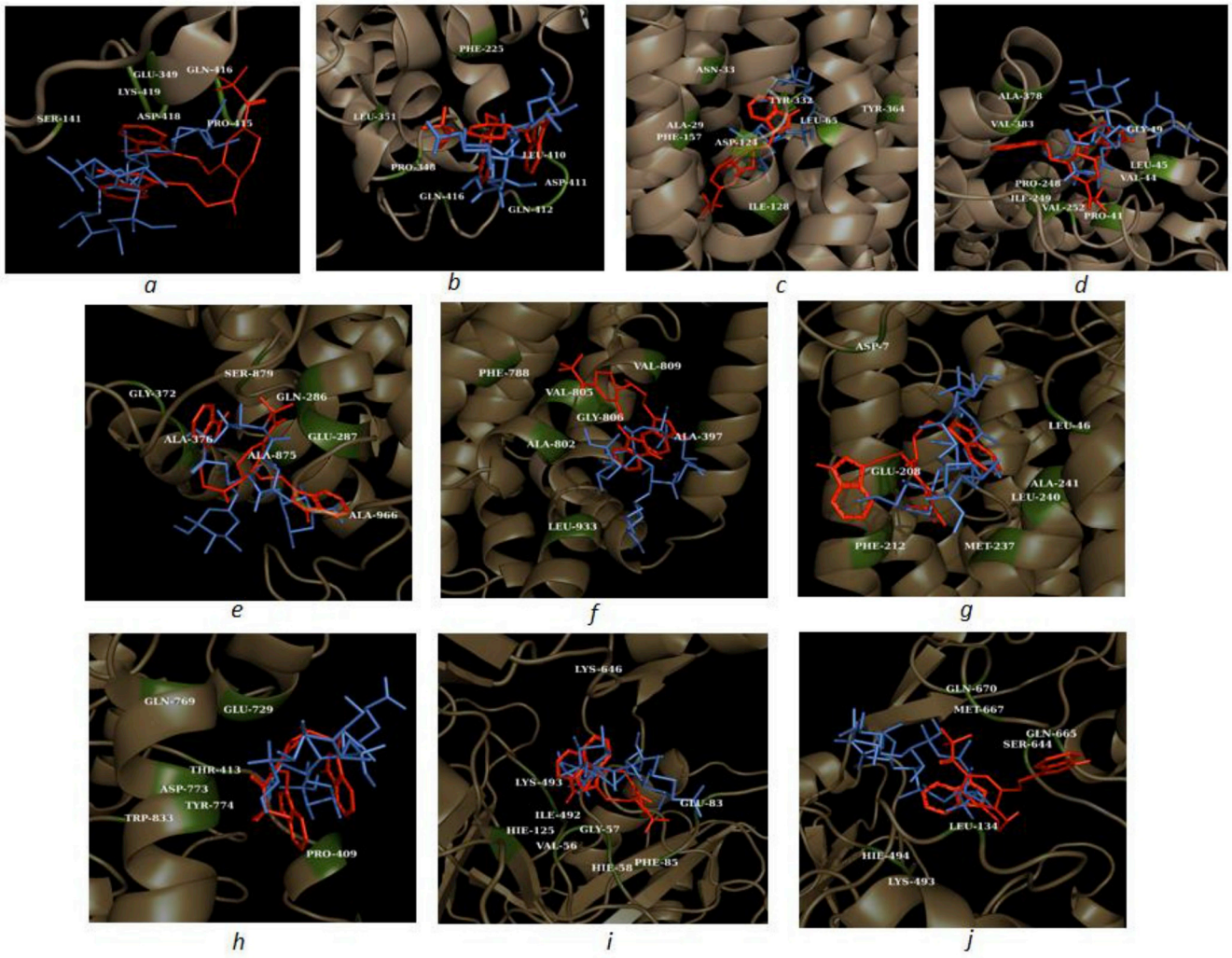

Fig. 6. Slice docking: Binding sites at Tap (*a* site 1, *b* site 2, *c* site 3 and *d* site 4), and MmpL5 (*e* site 1, *f* site 2, *g* site 3, *h* site 5, *i* site 7 and *j* site 8) (both models in cartoon) for Clarithromycin (blue sticks) and NUNM01 (red sticks). Some of the protein residues contacted, depicted in green in the cartoon representation, are listed for the respective panels (refer to Tables 7 and 8 for a complete list): (a) SER serine 141, GLU glutamic acid 349, PRO proline 415, GLN glutamine 416, ASP aspartic acid 418, LYS lysine 419; (b) PHE phenylalanine 225, PRO proline 348, LEU leucine 351, LEU leucine 410, ASP aspartic acid 411, GLN glutamine 412, GLN glutamine 416; (c) ALA alanine 29, ASN aspargine 33, LEU leucine 65, ASP aspartic acid 124, ILE isoleucine 128, PHE phenylalanine 157, TYR tyrosine 332, TYR tyrosine 364; (d) PRO proline 41, VAL valine 44, LEU leucine 45, GLY glycine 49, PRO proline 248, ILE isoleucine 249, VAL valine 252, ALA alanine 378, VAL valine 383; (e) GLN glutamine 286, GLU glutamic acid 287, GLY glycine 372, ALA alanine 376, ALA alanine 875, SER serine 879, ALA alanine 966; (f) ALA alanine 397, PHE phenylalanine 788, ALA alanine 802, VAL valine 805, GLY glycine 806, VAL valine 809, LEU leucine 933; (g) ASP aspartic acid 7, LEU leucine 46, GLU glutamic acid 208, PHE phenylalanine 212, MET methionine 237, LEU leucine 240, ALA alanine 241; (h) THR threonine 413, GLU glutamic acid 729, GLN glutamine 769, ASP aspartic acid 773, TYR tyrosine 774, TRP tryptophan 833, PRO proline 409; (i) VAL valine 56, GLY glycine 57, HIE histidine 58, GLU glutamic acid 83, PHE phenylalanine 85, HIE histidine 125, ILE isoleucine 492, LYS lysine 493, LYS lysine 646; (j) LEU leucine 134, LYS lysine 493, HIE histidine 494, SER serine 644, GLN glutamine 665, MET methionine 667, GLN glutamine 670. (For interpretation of the references to color in this figure legend, the reader is referred to the Web version of this article.)

Minimization with Amber 14 [31], using force field ff14SB [32], was performed in two stages. For each solvated complex, the protein and counterions were constrained while water molecules were relaxed with 1500 steps of steepest-descent minimization followed by 500 steps of conjugate gradient minimization using an 8 Å nonbonded cutoff. Next, the full system of the structure with solvent and counterions, was relaxed with 2000 steps of steepest-descent and 1000 steps of conjugate-gradient minimization using an 8 Å nonbonded cutoff.

The molecular structures of the THP (NUNM01, NUNM08, NUNM09 and NUNM11) were made and geometrically optimized with the software Avogadro [33], while structures for CLA, CCCP and VP were downloaded from PubChem (CIDs 84029, 2520 and 2603, respectively) [34].

AutodockTools4 [35] was used to prepare the molecular structures (proteins and ligands) and generate the files needed to obtain the FEBs through docking simulations in Autodock Vina [36]. In all docking simulations ligands were allowed to have torsions but the protein models were considered rigid. The protein residues contacted by the ligands were obtained with LigPlot+ with default parameters [37].

2.9. Docking simulations

We used two distinct docking techniques: blind docking [38] and slice docking [13].

2.9.1. Blind docking

Primarily, blind docking runs were conducted for the MmpL5 and Tap models to verify whether the NUNM compounds were comparable to VP, CCCP and EtBr regarding docking sites and FEB magnitudes. The Autodock Vina exhaustiveness parameter was set to 500 due to the

Table 7
Slice Docking. Protein residues contacted by the ligands NUNM01, clarithromycin, verapamil, ethidium bromide and carbonyl cyanide *m*-chlorophenyl hydrazone at the binding sites on MmpL5.

Slice Docking – MmpL5														
	Site 1					Site 4					Site 7			
NUNM01	CLA	VP	EtBr	CCCP	NUNM01	CLA	VP	EtBr	CCCP	NUNM01	CLA	VP	EtBr	CCCP
GLN 286	X	X	X	–	–	VAL 199	–	–	–	VAL 56	X	X	X	–
GLU 287	X	X	X	–	–	ASP 202	–	–	–	GLY 57	X	X	X	–
ARG 290	X	X	X	–	–	LEU 206	–	–	–	HIE 58	X	X	–	–
VAL 367	X	X	–	–	–	GLN 424	–	–	–	GLU 83	X	X	X	–
GLY 372	X	X	–	–	–	VAL 425	–	–	–	PHE 85	X	X	X	–
ALA 373	X	X	–	–	–	GLN 508	–	–	–	HIE 125	X	X	–	–
ALA 376	X	X	–	–	–	LEU 510	–	–	–	GLN 127	–	X	–	–
ARG 857	X	–	–	–	–	GLY 894	–	–	–	ILE 492	X	–	X	–
ARG 872	X	X	–	–	–	VAL 897	–	–	–	LYS 493	X	X	X	–
ALA 875	X	X	X	–	–	SER 898	–	–	–	LYS 646	X	X	X	–
SER 879	X	X	X	–		Site 5					Site 8			
ALA 963	X	–	X	–	NUNM01	CLA	VP	EtBr	CCCP	NUNM01	CLA	VP	EtBr	CCCP
VAL 964	X	–	X	–	LEU 408	–	X	–	X	PHE 129	–	X	X	X
ARG 965	X	–	–	–	PRO 409	X	X	X	–	LEU 134	X	X	X	X
ALA 966	X	X	X	–	THR 413	X	X	X	–	LYS 493	X	–	X	–
	Site 2				GLU 729	X	X	X	–	HIE 494	X	X	X	–
NUNM01	CLA	VP	EtBr	CCCP	GLN 769	X	X	X	–	SER 644	X	X	–	–
ALA 397	X	X	X	–	ASP 773	X	X	X	X	ASP 664	–	X	X	X
PHE 788	X	–	–	–	TYR 774	X	X	X	X	GLN 665	X	X	X	X
ALA 802	X	–	X	–	TRP 833	X	X	X	X	THR 666	–	X	X	–
VAL 805	X	–	X	–		Site 6				MET 667	X	–	–	X
GLY 806	X	X	X	–	NUNM01	CLA	VP	EtBr	CCCP	GLN 670	X	X	X	–
VAL 809	X	–	–	–	–	ASP 11	–	X	–					
ILE 929	–	X	–	–	–	ALA 12	X	X	–					
LEU 933	X	X	X	–	–	PHE 13	–	X	–					
	Site 3				–	PRO 14	X	X	–					
NUNM01	CLA	VP	EtBr	CCCP	–	VAL 49	X	X	–					
ASP 7	X	X	–	–	–	VAL 50	X	X	–					
LEU 46	X	X	X	X	–	PRO 51	–	–	–					
GLU 205	–	X	–	–	–	GLN 52	X	–	–					
GLU 208	X	–	X	X	–	MET 72	–	–	–					
PHE 212	X	–	X	X	–	HIE 122	X	–	–					
MET 237	X	X	X	X	–	GLN 157	X	–	–					
LEU 240	X	X	X	X	–	GLU 159	X	X	–					
ALA 421	X	–	X	X	–	SER 251	X	X	–					

The residues contacted by NUNM01 are listed at the first column, the "X", if present, indicates that the other compounds also contact these residues. CCCP Carbonyl cyanide *m*-chlorophenyl hydrazone, VP verapamil, EtBr ethidium bromide, CLA clarithromycin, ALA alanine, ASN aspargine, GLY glycine, GLN glutamine, GLU glutamic acid, HIE histidine, ILE isoleucine, LEU leucine, LYS lysine, PHE phenylalanine, PRO proline, SER serine, THR threonine, TYR tyrosine, TRP tryptophan, VAL valine.

large volume of the search box (dimensions in the *x*, *y* and *z* axes of 118 x 102 × 110 Å for MmpL5 and 74 x 92 × 66 Å for Tap). Six binding sites for MmpL5 and three for Tap, were selected considering the highest magnitude FEB values. When blind docking detected CCCP or VP, with a significant FEB in a site not occupied by any NUNM, we docked the NUNM at this specific region.

2.9.2. Slice docking

Since it is still unknown whether CLA is transported by MmpL5 and Tap, to verify a possible affinity between this compound and the modeled protein structures, we used the technique of slice docking as described previously [13]. In these simulations, CLA was chosen as the reference to compare the other ligands to, because it is the main antimicrobial used in the treatment of infections caused by *M. abscessus* and we wanted to verify whether, *in silico*, the NUNM compounds and CLA would compete for the same binding sites, with comparable FEBs at the modeled structures of MmpL5 and Tap. The Autodock Vina exhaustiveness parameter was set to 128 because the volume of the virtual search box was much smaller than that for blind docking. MmpL5 was divided into 8 slices, each with dimensions in the *x*, *y* and *z* planes of 92 x 26 × 92 Å. For each slice we identified the highest FEB for CLA. Tap was divided into 5 slices with dimensions of 68 x 26 × 64 Å. The slices in both models had sizes that were able to accommodate the ligands in any configuration and spatial orientation. Five sites of affinity were chosen. We then slice-docked the compounds NUNM, VP, CCCP and EtBr in the MmpL5 and Tap models to verify whether they could compete with CLA for the same binding sites, with FEB magnitudes comparable to or higher than those of CLA.

3. Results

3.1. Antimicrobial activity

According to the observed MIC values (Table 1), the strain used in this study was susceptible to AMI and CIP, and presented induced resistance to CLA at day 7 of incubation. The MIC for the THP compounds varied between 25 μg/mL and 100 μg/mL, however; NUNM02 and NUNM06 showed MIC > 200 μg/mL and consequently were excluded from the next steps. We observed no cytotoxicity of the NUNM compounds ($IC_{50} \geq 200$ μg/mL).

Table 8
Slice Docking. Protein residues contacted by the ligands NUNM01, clarithromycin, verapamil, ethidium bromide and carbonyl cyanide *m*-chlorophenyl hydrazone at the binding sites on Tap.

Slice Docking – Tap

	Site 1					Site 4			
N1	CLA	VP	EtBr	CCCP	N1	CLA	VP	EtBr	CCCP
ALA 139	–	–	X	–	–	ILE 31	–	X	–
SER 141	X	X	X	X	–	LEU 167	–	X	–
PRO 348	–	X	–	–	–	LEU 171	–	X	–
GLU 349	X	X	X	–	–	TRP 182	–	X	–
GLN 412	–	–	X	–	–	ALA 186	–	X	–
PRO 415	X	X	X	X		Site 5			
GLN 416	X	–	–	–	N1	CLA	VP	EtBr	CCCP
ASP 418	X	–	X	X	PRO 41	X	X	X	X
LYS 419	X	X	X	X	VAL 44	X	X	–	–
	Site 2				LEU 45	X	X	X	X
N1	CLA	VP	EtBr	CCCP	GLY 49	X	X	X	–
PHE 225	X	–	–	–	ALA 54	–	X	–	X
ARG 346	–	X	–	X	PRO 248	X	X	X	X
PR0 348	X	X	–	X	ILE 249	X	–	X	X
LEU 351	X	X	–	–	GLU 250	–	X	X	–
LEU 410	X	–	–	–	VAL 252	X	X	X	X
ASP 411	X	–	–	X	LEU 254	–	X	–	X
GLN 412	X	X	–	X	PRO 255	–	X	–	–
GLN 416	X	X	–	X	ALA 374	–	X	–	–
	Site 3				ALA 378	X	X	X	–
N1	CLA	VP	EtBr	CCCP	VAL 383	X	X	X	–
LEU 22	–	–	–	X					
SER 26	–	X	–	X					
ALA 29	X	X	–	–					
ASN 33	X	X	–	–					
LEU 65	X	–	–	–					
ASP 124	X	X	–	–					
GLY 127	–	X	–	–					
ILE 128	X	X	–	–					
ARG 131	–	–	–	X					
GLU 132	–	–	–	X					
TYR 153	–	–	–	X					
GLU 154	–	X	–	–					
PHE 157	X	X	–	X					
TYR 332	X	X	X	–					
TYR 364	X	X	–	–					

The residues contacted by NUNM01 are listed at the first column, the "X", if present, indicates that the other compounds also contact these residues. CCCP Carbonyl cyanide *m*-chlorophenyl hydrazone, VP verapamil, EtBr ethidium bromide, CLA clarithromycin, ALA alanine, ARG arginine, ASN aspargine, GLY glycine, GLN glutamine, GLU glutamic acid, ILE isoleucine, LEU leucine, LYS lysine, PHE phenylalanine, PRO proline, SER serine, TYR tyrosine, TRP tryptophan, VAL valine.

3.2. Modulatory effect of efflux inhibitors

The nine THPs that showed some antimicrobial activity (MIC $< 100\,\mu g/mL$) were evaluated as EI, and compared to the canonical inhibitors CCCP and VP. The MF that quantified the reduction of MIC values in the presence of the EI is depicted in Table 2.

A four-fold reduction of the AMI and CLA MIC values in the presence of CCCP and VP (MF = 4) was observed. In addition, in the presence of NUNM01, the MICs of AMI, CIP and CLA were reduced by 4, 4, and 16-fold, respectively. The MIC of CLA was reduced 8-fold in the presence of NUNM08 and NUNM11 and 16-fold in the presence of NUNM09.

3.3. EtBr accumulation assay

To confirm and visualize the efflux-inhibitory activity of the four THPs (NUNM01, NUNM08, NUNM09 and NUNM11) that had a MF > 4, the fluorometric technique in the presence of the universal efflux substrate EtBr was carried out in an Infinite F200 fluorimeter. As shown in Fig. 2, the effect of each EI on the accumulation of EtBr in the ATCC 19977 strain was observed and the RFF was calculated. In this study, the EI that presented the highest EtBr accumulation rate was the THP compound, NUNM01 (RFF = 3.1), followed by NUNM09 (RFF = 1.8), NUNM11 (RFF = 1.7), NUNM08 (RFF = 1.2) and the EI VP (RFF = 1.1) and CCCP (RFF = 0.4).

3.4. Computer simulations

3.4.1. Blind docking

To the four THP compounds that showed a significantly elevated MF (> 4) and associated high RFF, molecular modeling simulations for the *M. abscessus* modeling proteins were performed to better understand of the efflux mechanism. These docking simulations revealed possible binding sites for the ligands on the structures of the MmpL5 and Tap efflux-pumps. In the blind docking assays, we considered six sites on MmpL5 and three on Tap (Fig. 3a and b). The NUNM molecules had higher magnitude FEBs than VP and CCCP at these sites (Table 3), which suggests that these THP compounds could be considered EI.

For the MmpL5 model, the simulations did not dock CCCP at site 1 or 3, EtBr at site 3 or 5 or VP at site 6. For Tap, CCCP did not dock at site 1 of the modeled structure (Table 3), but at a nearby position. In spite of being off site 1, it had four common residues with NUNM01 (alanine 286, tyrosine 285, glycine 333 and proline 337).

Fig. 4 shows in detail the six (MmpL5) and three (Tap) binding sites for NUNM01, CCCP, VP and EtBr, illustrating also the protein residues contacted by all the ligands at the respective binding sites. In MmpL5, as can be seen in Table 3, all ligands docked successfully at site 1 except CCCP; however, CCCP contacted the protein residues glutamine 286 and serine 879, which were also contacted by NUNM01, VP and EtBr at this site. All ligands tested had affinity for sites 2 and 4. These were sites of high magnitude FEB for the NUNM compounds, especially NUNM01. The FEB values were higher for NUNM01 in all cases, suggesting that, if MmpL5 is involved in antimicrobial transport, NUNM01 is possibly an efflux inhibitor. For Tap, NUNM01 had the highest magnitude FEB at the three binding sites proposed. Interestingly, CCCP, VP and EtBr, for all binding sites described by the blinding docking runs for both structures MmpL5 and Tap, always had a smaller FEB than those of NUNM01. Tables 5 and 6 list, for the blind docking runs, the protein residues contacted by NUNM01, VP, EtBr and CCCP on Mmpl5 and Tap.

3.4.2. Slice docking

The procedure resulted in eight sites of good affinity distributed along MmpL5 and five sites along Tap (Fig. 5a and b). In these binding sites, these simulations revealed that the CLA FEB values were actually slightly higher in magnitude than those computed for VP and CCCP (Table 4), showing that *in silico*, CLA had a good affinity for the Mmpl5 and Tap models, suggesting that these transporters could participate in the efflux process. These sites do not necessarily correspond to the sites found by blind docking, depicted in Fig. 3, because in the slice docking assays, the binding sites of CLA were considered as the reference. These slice dockings revealed direct competition between the NUNM compounds and CLA for the same binding sites. The NUNM FEB magnitudes were generally (not always) higher than those of CLA, VP, CCCP and EtBr. On MmpL5, only CLA was found at binding site 4. In addition, NUNM01, NUNM11 and CCCP did not dock at site 6. On Tap, only CLA and EtBr docked at site 4, with FEB values of −5.9 and −7.2 kcal/mol, respectively. Fig. 6 shows NUNM01 competing with CLA at the binding sites found for the MmpL5 and Tap models.

In all docking runs (blind or slice) performed in this study, the NUNM molecules were able to compete for binding sites with CLA, CCCP, VP and EtBr, with significant FEB values. In addition, it is important to point out that in this study NUNM01 always had the best FEB

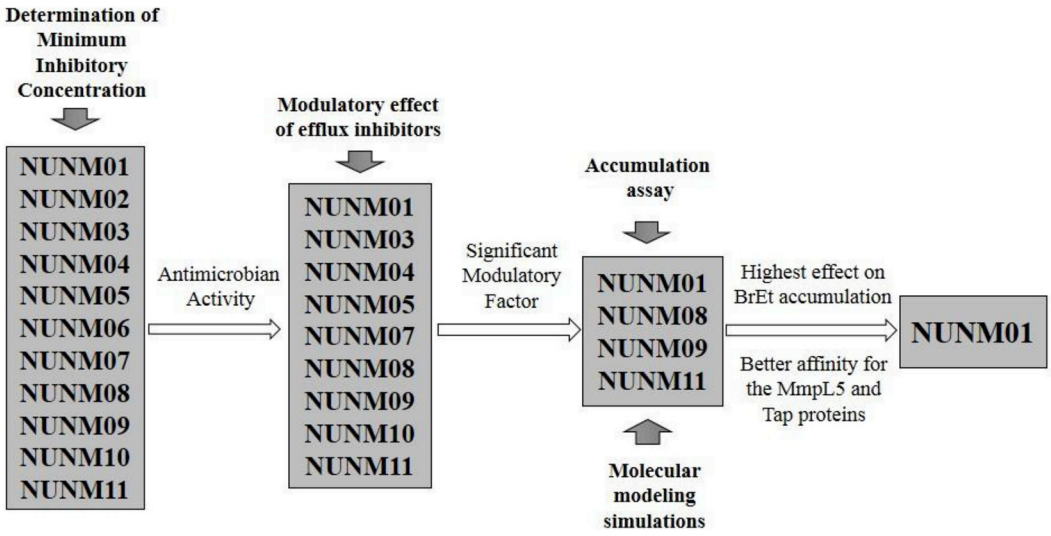

Fig. 7. Screening scheme of tetrahydropirydines compounds.

values among all the ligands at the binding sites identified for the MmpL5 and Tap models (Tables 3 and 4). Tables 7 and 8 list, for the slice docking runs, the protein residues contacted by NUNM01, CLA, VP, EtBr and CCCP on Mmpl5 and Tap.

4. Discussion

Previously, compounds containing the THP nucleus have demonstrated a comprehensive variety of pharmacological activities, including antimicrobial activity [39]. In this study, 11 THP compounds differing in the structures of radicals 1 and 2 were evaluated *in vitro* and *in silico*, of which nine showed antimicrobial activity at ≤ 100 μg/mL concentration.

In addition, assessing the antimicrobial activity, we aimed to evaluated these nine THPs as EI, and we found a significant reduction in the MICs of AMI, CIP and CLA in the presence of NUNM01, NUNM08, NUNM09 or NUNM11, with MF ≥ 4 and RFF > 1, indicating effective synergistic activity via efflux inhibition [21]. Notably, NUNM01 had the highest RFF result with the highest MF among all the EI tested in this study.

Interestingly, NUNM01 is the only compound that has two indoles in the R1 and R2 positions attached to the THP structure. The indole radical can be found in various organic compounds, such as alkaloids, that have potent antibacterial activity and have been described as efflux inhibitors [40,41]. In addition, indoles constitute a heterocyclic ring system with a molecular architecture that makes them suitable candidates for drug development [42].

Computational simulations revealed possible binding sites for the ligands on MmpL5 and Tap protein structures. These transporters are known multidrug resistance pumps in *Mycobacterium* spp., conserved in the *M. tuberculosis* complex and *M. avium* [43–45]. The ligands CCCP and VP are known efflux pump inhibitors in mycobacteria, and EtBr is a universal substrate of many efflux pumps that has been used in accumulation assays in several studies [22,46,47].

The NUNM preferences for the same sites, with a FEB of higher magnitude than those of CCCP, VP (except for NUNM08 in site 2) and EtBr demonstrated, *in silico*, a plausible affinity of the NUNM compounds for these sites. Although it is unknown which pumps in *M. abscessus* subsp. *abscessus* take part in the drug efflux, and our docking simulations suggested that MmpL5 and Tap could be involved in the process. NUNM01 had common preferences for binding sites with VP and competes directly with binding sites preferred by CLA. These *in silico* results suggest that NUNM01 could be a potential inhibitor of CLA efflux. In fact, the supposed participation of MmpL5 in the efflux process is reinforced by a recent *in vitro* study in which Halloum et al. (2017) [7] showed that mutations in the MmpL cognate transcriptional regulators represent an important drug resistance mechanism involving the MmpS5-MmpL5 system in *M. abscessus*.

THP compounds may provide an excellent pharmacophore for the development of novel combinational therapies using efflux pump inhibitors against drug resistance in *M. abscessus* [13,48]. NUNM01 is the ideal candidate EI in *M. abscessus,* as it possibly inhibit the activity of the MmpL5 and Tap efflux pumps. Fig. 7 shows the screening scheme that highlighted this THP compound as the best inhibitor of the efflux mechanism.

Acknowledgments

Special thanks to the Universidade Federal de Rio Grande for the structural support needed for developing the study, and Fundação Oswaldo Cruz for granting the *M. abscessus* strains.

Appendix A. Supplementary data

Supplementary data to this article can be found online at https://doi.org/10.1016/j.tube.2019.07.004.

Funding

Coordenação de Aperfeiçoamento de Pessoal de Nível Superior' (CAPES, MEC, Brazil) for financial support to I. B. R and M.V. through the "Ciências em Fronteiras/Professor Visitante Especial" program (Projeto **88881.064961/2014–01** - Jose R. Lapa e Silva/UFRJ coordinator).

References

[1] Griffith De, Aksamit T, Brown-Elliott Ba, Catanzaro A, Daley C, Gordin F, Holland Sm, Horsburgh R, Huitt G, Iademarco Mf, Iseman M, Olivier K, Ruoss S, Von Reyn Cf, Wallace Jr. Rj, Winthrop K. An official ats/idsa statement: diagnosis, treatment, and prevention of nontuberculous mycobacterial diseases. Am J Respir Crit Care Med 2007;175:367–416.

[2] Koh Wj, Stout Je, Yew Ww. Advances in the management of pulmonary disease due to *Mycobacterium abscessus* complex. Int J Tuberc Lung Dis 2014;18:1141–8.

[3] Lee Jh, Lee J. Indole as an intercellular signal in microbial communities. FEMS Microbiol Rev 2010;34:426–44.

[4] Nash Ka, Brown-Elliott Ba, Wallace Jr. Rj. A novel gene, erm(41), confers inducible macrolide resistance to clinical isolates of *Mycobacterium abscessus* but is absent from *Mycobacterium chelonae*. Antimicrob Agents Chemother 2009;53:1367–76.

[5] Chancey St, Dorothea Zähner D, Stephens Ds. Acquired inducible antimicrobial resistance in Gram-positive bacteria. Future Microbiol 2012;7:959–78.

[6] Carvalho Nfg, Sato Dn, Pavan Fr, Ferrazoli L, Chimara E. Resazurin microtiter assay for clarithromycin susceptibility testing of clinical isolates of *Mycobacterium abscessus* group. J Clin Lab Anal 2016;30:751–5.

[7] Halloum I, Viljoen A, Khanna V, Craig D, Bouchier C, Brosch R, Coxon G, Kremera L. Resistance to thiacetazone derivatives active against *Mycobacterium abscessus* involves mutations in the Mmpl5 transcriptional repressor Mab_4384 antimicrob agents. Chemotherapy 2017;61:2509–16.

[8] Esteban J, Martín-De-Hijas Nz, Ortiz A, Kinnari Tj, Sánchezab Gadea I, Fernández-Roblas R. Detection of *lfra* and *tap* efflux pump genes among clinical isolates of non-pigmented rapidly growing mycobacteria. Int J Antimicrob Agents 2009;34:454–6.

[9] schmalstieg Am, srivastava S, belkaya S, deshpande D, meek C, leff R, van Oers Ns, gumbo T. The antibiotic resistance arrow of time: efflux pump induction is a general first step in the evolution of mycobacterial drug resistance. Antimicrob Agents Chemother 2012;56:4806–15.

[10] Marquez B. Bacterial efflux systems and efflux pumps inhibitors. Biochimie 2005;87:1137–47.

[11] Lomovaskwaya O, Warren Ms, Lee A, Galazzo J, Fronko R, Lee M, Blais J, Cho D, Chamberland S, Renau T, Leger R, Hecker S, Watkins W, Hoshino K, Ishida H, Lee Vj. Identification and characterization of inhibitors of multidrug resistance efflux pumps in *Pseudomonas aeruginosa*: novel agents for combination therapy. Antimicrob Agents Chemother 2001;45:105–16.

[12] Taylor Md, Badger Ew, Steffen Rp, Haleen Sj, Pugsley Ta, Shih Yh, et al. 2-(2-Aryl-2-oxoethylidene)-1,2,3,4-Thps. Novel isomers of 1,4-dihydropyridine calcium channel blockers. J Med Chem 1998;31:1659–64.

[13] Silva Jr. L, Carrion Ll, Von Groll A, Costa Ss, Junqueir E, Ramos Df, Cantos J, Seus Vr, Couto I, Fernandes Ls, Bonacorso Hg, Map Martins, Zanatta N, Viveiros M, Machado Ks, Silva Pea. In vitro and in silico analysis of the efficiency of tetrahydropyridines as drug efflux inhibitors in *Escherichia coli*. Int J Antimicrob Agents 2017;49:308–14.

[14] Meng Xy, Zhang Hx, Mezei M, Ciu M. Molecular docking: a powerful approach for structure-based drug discovery. Curr Comput Aided Drug Des 2011;7:146–57.

[15] Clinical And Laboratory Standards Institute. Susceptibility testing of mycobacteria, nocardiae, and other aerobic actinomycetes; approved standard. second ed. Clsi document M24-A2 2011;31:1–76.

[16] Zanatta N, Lobo MM, Santos JS, Souza LA, Andrade VP, Banacorso HG, et al. Synthesis of 1-Arylethyl-2-arylethylamino-5-trifluoroacetyl-1,2,3,4-tetrahydropyridines and potential cell efflux pump inhibition related compounds. J Heterocyclic Chem 2014:1–6. https://doi.org/10.1002/jhet.2271.

[17] Ramis Ib, Cnockaert M, Von Groll A, Nogueira Cl, Leão Sc, Andre E, Simon A, Palomino Jc, Da Silva Pe, Vandamme P, Martin A. Antimicrobial susceptibility of rapidly growing mycobacteria using the rapid colorimetric method. Eur J Clin Microbiol Infect Dis 2015;34:1403–13.

[18] Palomino Jc, Martin A, Camacho M, Guerra H, Swings J, Portaels F. Resazurin microtiter assay plate: simple and inexpensive method for detection of drug resistance in *Mycobacterium tuberculosis*. Antimicrob Agents Chemother 2002;46:2720–2.

[19] Ahmed Sa, Gogal Rm, Walsh Jr. Je. A new rapid and simple non-radioac- tive assay to monitor and determine the proliferation of lymphocytes: an alternative to [3h] thymidine incorporation assay. J Immunol Methods 1994;170:211–24.

[20] Snewin Va, Gares Mp, Gaora Po, Hasan Z, Brown In, Young Db. Assess- ment of immunity to mycobacterial infection with luciferase reporter constructs. Infect Immun 1999;67:4586–93.

[21] Groblacher B, Kunert O, Bucar F. Compounds of Alpinia katsumadai as potential efflux inhibitors in *Mycobacterium smegmatis*. Bioorg Med Chem 2012;20:2701–6.

[22] coelho T, machado D, couto I, maschmann R, ramos D, von Groll A, rossetti Ml, silva Pa, viveiros M. Enhancement of antibiotic activity by efflux inhibitors against multidrug resistant *Mycobacterium tuberculosis* clinical isolates from Brazil. Front Microbiol 2015;6:1–12.

[23] Ramis Ib, Vianna Js, Reis Aj, Von Groll A, Ramos Df, Viveiros M, Silva Pea. Antimicrobial and efflux inhibitor activity of usnic acid against *Mycobacterium abscessus*. Planta Med 2018;84:1265–70.

[24] Paixão L, Rodrigues L, Couto I, Martins M, Fernandes P, Carvalho Cccr, Monteiro Ga, Sansonetty F, Amaral L, Viveiros M. Fluorometric determination of ethidium bromide efflux kinetics in *Escherichia coli*. J Biol Eng 2009;3:18.

[25] Viveiros M, Rodrigues L, Martins M, Couto I, Spengler G, Martins A, Amaral L. Evaluation of efflux activity of bacteria by a semi-automated fluorometric system. Methods Mol Biol 2010;642:159–72.

[26] Machado D, Coelho T, Perdigão J, Pereira C, Couto I, Portugal I, Maschmann R, Ramos D, Von Groll A, Rossetti Mlr, Silva Pa, Viveiros M. Interplay between mutations and efflux in drug resistant clinical isolates of *Mycobacterium tuberculosis*. Front Microbiol 2017;8:1–18.

[27] Home Genbank. Available at: https://www.ncbi.nlm.nih.gov/genbank/, Accessed date: 2 November 2017.

[28] Nih. membrane protein mmpl5 [Mycobacterium abscessus subsp. abscessus] - protein - Ncbi Available at: https://www.ncbi.nlm.nih.gov/protein/Slk97379, Accessed date: 30 April 2018.

[29] Putative Nih. Drug antiporter protein precursor [Mycobacterium abscessus su - protein - Ncbi Available at: https://www.ncbi.nlm.nih.gov/protein/Sij44512.1, Accessed date: 30 April 2018.

[30] kelley La, mezulis S, yates Cm, wass Mn, sternberg Mj. The Phyre2 web portal for protein modeling, prediction and analysis. Nat Protoc 2015;10:845–58.

[31] Case Da, et al. Amber 14. 2014.

[32] Maier Ja, martinez C, kasavajhala K, wickstrom L, hauser Ke, simmerling C. ff14sb: improving the accuracy of protein side chain and backbone parameters from ff99sb. J Chem Theory Comput 2015;11:3696–713.

[33] Hanwell Md, curtis De, lonie Dc, vandermeersch T, zurek E, hutchison Gr. Avogadro: an advanced semantic chemical editor, visualization, and analysis platform. J Cheminf 2012;4:17.

[34] Pubchem project Available at: https://pubchem.ncbi.nlm.nih.gov/, Accessed date: 30 March 2018.

[35] Morris G, Huey R. Autodock 4 and Autodocktools4: automated docking with selective receptor flexibility. J Comput Chem 2009;30:2785–91.

[36] Trott O, Olson Aj. Autodock Vina: improving the speed and accuracy of docking with a new scoring function, efficientoptimization, and multithreading. J Comput Chem 2010;31:455–61.

[37] Wallace AC, Laskowski RA, Thornton JM. Ligplot: a program to generate schematic diagrams of protein-ligand interactions. Protein Eng 1995;8:127–34.

[38] Hetényi C, Van Der Spoel D. Blind docking of drug-sized compounds to proteins with up to a thousand residues. FEBS Lett 2006;580:1447–50.

[39] zhou Yh, fu H, zhao Wx, chen Wl, su Cy, sun H, ji Ln, mao Zw. Synthesis, structure, and activity of supramolecular mimics for the active site and arg 141 residue of copper, zinc-superoxide dismutase. Inorg Chem 2007;46:734–9.

[40] Cushinie Ttp, Cushinie B, Lamb Aj. Alkaloids: an overview of their antibacterial, antibiotic-enhancing and antivirulence activities. Int J Antimicrob Agents 2014;44:377–86.

[41] Zhu T, Cleaver L, Wang W, Podoll Jd, Walls S, Jolly A, Wang X. Tetracyclic indolines as a novel class of b-lactam-selective resistance-modifying agent for Mrsa. Eur J Med Chem 2017;125:130–42.

[42] Chadha, Silakari. Indoles as therapeutics of interest in medicinal chemistry: bird's eye view. Eur J Med Chem 2017;134:159–84.

[43] Silva Pea, Von Groll A, Martin A, Palomino Jc. Efflux as a mechanism for drug resistance in *Mycobacterium tuberculosis*. FEMS Immunol Med Microbiol 2011;63:1–9.

[44] Briffotaux J, Huang W, Wang X, Gicquel B. Mmps5/Mmpl5 as an efflux pump in Mycobacterium species. Tuberculosis 2017;107:13–9.

[45] Nasiri Mj, Haeili M, Ghazi M, Goudarzi H, Pormohammad A, Fooladi Aai, Feizabadi Mm. New insights in to the intrinsic and acquired drug resistance mechanisms in mycobacteria. Front Microbiol 2017;8:1–19.

[46] Pule Cm, Sampson Sl, Warren Rm, Black Pa, Van Helden Pd, Victor Tc, Louw Ge. Efflux pump inhibitors: targeting mycobacterial efflux systems to enhance Tb therapy. J Antimicrob Chemother 2016;71:17–26.

[47] jaiswal I, jain A, verma Sk, singh P, kant S, singh M. Effect of efflux pump inhibitors on the susceptibility of *Mycobacterium tuberculosis* to isoniazid. Lung India 2017;34:499–505.

[48] vianna Js, ramis Ib, bierhals D, von Groll A, ramos Df, zanatta N, lourenço Mc, viveiros M, silva Pea. Tetrahydropyridine derivative as efflux inhibitor in *Mycobacterium abscessus*. J Glob Antimicrob Resist 2019;17:296–9.